A comparison of spatial sampling techniques enabling first principles modeling of a synthetic aperture RADAR imaging platform

Michael Gartley*[a], Adam Goodenough[a], Scott Brown[a], Russel P. Kauffman[b]
[a] Digital Imaging and Remote Sensing Laboratory, Rochester Institute of Technology,
54 Lomb Memorial Drive, Rochester, NY 14623-5604
[b] Lockheed Martin Information Systems and Global Services,
P.O. Box 8048, Philadelphia PA, 19101;

ABSTRACT

Simulation of synthetic aperture radar (SAR) imagery may be approached in many different ways. One method treats a scene as a radar cross section (RCS) map and simply evaluates the radar equation, convolved with a system impulse response to generate simulated SAR imagery. Another approach treats a scene as a series of primitive geometric shapes, for which a closed form solution for the RCS exists (such as boxes, spheres and cylinders), and sums their contribution at the antenna level by again solving the radar equation. We present a ray-tracing approach to SAR image simulation that treats a scene as a series of arbitrarily shaped facetized objects, each facet potentially having a unique radio frequency optical property and time-varying location and orientation. A particle based approach, as compared to a wave based approach, presents a challenge for maintaining coherency of sampled scene points between pulses that allows the reconstruction of an exploitable image from the modeled complex phase history. We present a series of spatial sampling techniques and their relative success at producing accurate phase history data for simulations of spotlight, stripmap and SAR-GMTI collection scenarios.

Keywords: Synthetic aperture RADAR, modeling, simulation, phenomenology, sampling.

1. INTRODUCTION

Within the civil and defense remote sensing communities radiometric simulation of remotely-sensed scenes plays an important role in engineering trade studies, algorithm development and analyst training. Many software packages are capable of simulating focused synthetic aperture RADAR (SAR) imagery, such as Xpatch[1] and IRMA[2]. However, our understanding is these software packages have either limited or non-existent ability to simulate other modalities such as EO, IR, reflective and emissive polarimetric imagery, and LIDAR.

The Rochester Institute of Technology's Digital Imaging and Remote Sensing Laboratory develops the software code DIRSIG (Digital Image and Remote Sensing Image Generation) to simulate remotely sensed scenes across the 0.4 to 14 micron region of the electromagnetic spectrum with full spectral-polarimetric modeling capability. Recently DIRSIG has added a robust capability to model LIDAR collection platforms rigorously handling multiple bounce and moving geometry phenomenology. The one modality missing from the DIRSIG modeling capability is modeling signals, platforms, and antennas in the radio frequency (RF) region of the electromagnetic spectrum. This paper details our initial efforts to add SAR capability to DIRSIG, providing a truly multi-model modeling and simulation platform for the civil and defense remote sensing community.

2. TECHNICAL APPROACH

The DIRSIG model is an image generation tool that utilizes a complex computational radiometry sub-system to predict absolute fluxes within a 3D scene description. The model uses [1 x 4] Stokes vector and [4 x 4] Mueller matrix calculus to propagate, reflect, transmit, etc. fluxes within the simulated scene environment. The DIRSIG radiometry engine utilizes a single expression, governing equation across all wavelength regions such that reflected and self-emitted contributions are always included unless explicitly disabled.

Algorithms for Synthetic Aperture Radar Imagery XVII, edited by Edmund G. Zelnio, Frederick D. Garber,
Proc. of SPIE Vol. 7699, 76990N · © 2010 SPIE · CCC code: 0277-786X/10/$18 · doi: 10.1117/12.849552

The DIRSIG model has a flexible radiometry sub-system for computing radiance values for arbitrary paths within the defined scene. The primary mechanism used to predict images is reverse ray-tracing where rays originate from the imaging detectors and are propagated into the scene. When a ray intersects the scene geometry, the associated radiometry solver is run to compute the surface leaving radiance. DIRSIG has a handful of radiometry solvers used for opaque surfaces and the most flexible is the generic radiometry solver. The generic radiometry solver computes the reflected radiance by sampling the hemisphere above the target. The distribution of these samples is based on the shape and magnitude of the associated BRDF. The nominal hemispherical sampling is cosine projected and has user-defined sampling parameters (e.g. total number of samples, etc.). The incident loads for those samples are determined by tracing higher generation rays which intersect other surfaces and trigger other instances of the radiometry solver. The fidelity of the sampling for higher generation bounces can be decreased using a bounce-dependent decay rate that modifies the sampling parameters. The total number of bounces that are tracked is also user controllable. The incident loads from the sampled hemisphere are numerically integrated using the geometry specific reflectance (BRDF) and the solid angle of the sample.

2.1 Platform Motion

The traditional DIRSIG user interface is available to configure platform position, attitude and motion (Figure 1). The platform motion editor is capable of importing user specified 3D attitude and ephemeris data in earth-center-fixed (ECF), earth-north-up (ENU), or DIRSIG local scene coordinates. Alternatively, the platform motion editor has a static, spotlight and racetrack collection wizard to automatically generate ephemeris and attitude data over a finite time period. This configuration flexibility permits strip-map, spotlight and SAR-GMTI mode collections.

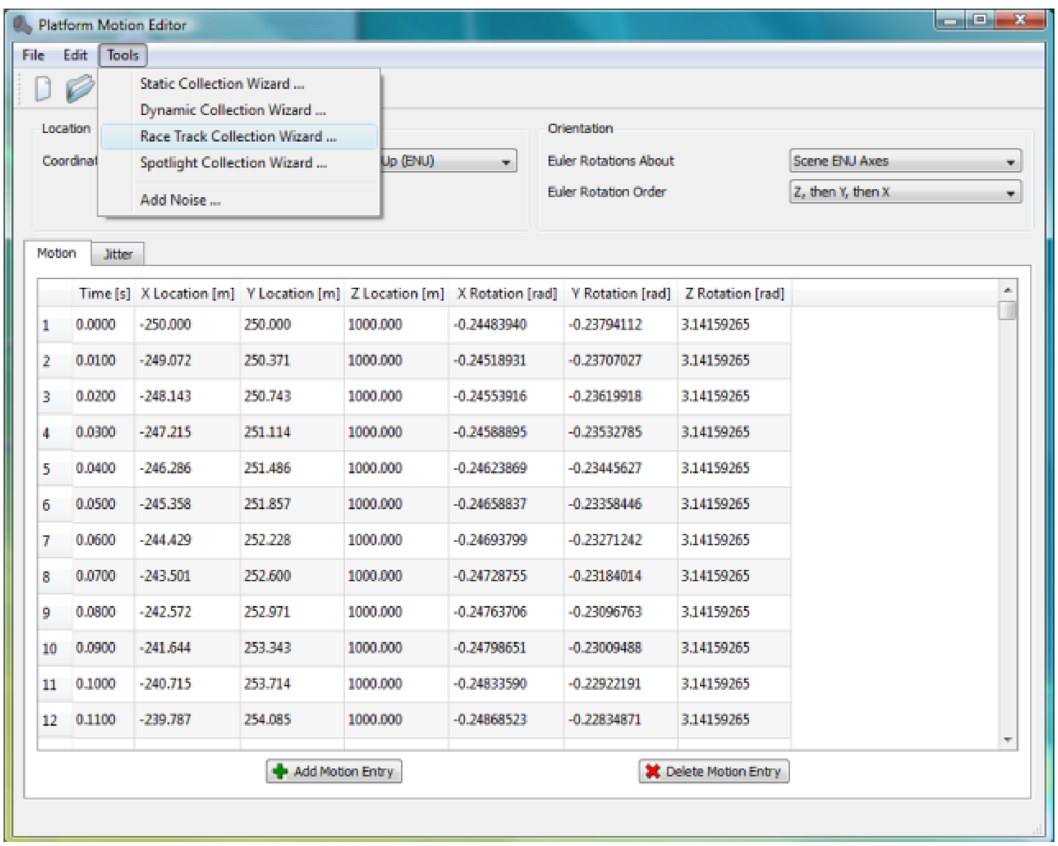

	Time [s]	X Location [m]	Y Location [m]	Z Location [m]	X Rotation [rad]	Y Rotation [rad]	Z Rotation [rad]
1	0.0000	-250.000	250.000	1000.000	-0.24483940	-0.23794112	3.14159265
2	0.0100	-249.072	250.371	1000.000	-0.24518931	-0.23707027	3.14159265
3	0.0200	-248.143	250.743	1000.000	-0.24553916	-0.23619918	3.14159265
4	0.0300	-247.215	251.114	1000.000	-0.24588895	-0.23532785	3.14159265
5	0.0400	-246.286	251.486	1000.000	-0.24623869	-0.23445627	3.14159265
6	0.0500	-245.358	251.857	1000.000	-0.24658837	-0.23358446	3.14159265
7	0.0600	-244.429	252.228	1000.000	-0.24693799	-0.23271242	3.14159265
8	0.0700	-243.501	252.600	1000.000	-0.24728755	-0.23184014	3.14159265
9	0.0800	-242.572	252.971	1000.000	-0.24763706	-0.23096763	3.14159265
10	0.0900	-241.644	253.343	1000.000	-0.24798651	-0.23009488	3.14159265
11	0.1000	-240.715	253.714	1000.000	-0.24833590	-0.22922191	3.14159265
12	0.1100	-239.787	254.085	1000.000	-0.24868523	-0.22834871	3.14159265

Figure 1. DIRSIG platform motion editor graphical user interface.

2.2 Antenna Configuration

Although no graphical user interface currently exists for setting up a SAR antenna, there exists a straightforward XML interface for doing so. The user may select either a circular dish, rectangular phased array style, or a notional perfectly uniform (rect function) angular gain pattern. The images in Figure 2 below demonstrate the angular pattern of a notional uniform and a phased array antenna and the resulting focused images of a point target (i.e. a corner reflector). The physical size of the transmit antenna and transmit power are specified within the same XML file framework. Additionally, the transmit carrier frequency, chirp rate and pulse length (which determine the transmission bandwidth) are specified within the XML antenna file framework. The number of Monte Carlo photons transmitted by the antenna can also be adjusted which determine the run time and fidelity of the final focused imagery.

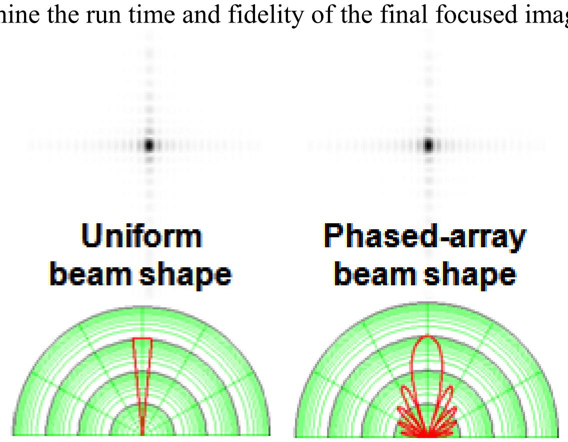

Figure 2. Examples of two beam patterns available within the DIRSIG SAR capability and the resulting response of a focused point target

2.3 Material Scattering Models

All of the legacy DIRSIG BRDF models are available to the RF / SAR user, however they may also pick from one or more of the new RF-specific scattering models. Traditionally in the RF literature, these models are cast in terms of Radar Cross Section (RCS) density (scattering cross section per unit area) or simply RCS which has units of area. For use within the DIRSIG radiometry framework, we have converted the RCS and RCS densities to effective bi-directional reflectance distribution function (BRDF) values via the relation:

$$BRDF = \frac{\sigma^0}{4\pi \cos\theta_i \cos\theta_r} \left[\frac{1}{sr}\right] \quad (1)$$

Where σ^0 is the RCS density [m^2/m^2] and θ_i and θ_r are the incident and reflected zenith angles respectively. DIRSIG supports ingestion of RCS density as a function of frequency that may be derived from measured values. Analytical models have some root in both theory and experimental measurements. DIRSIG supports the Constant Gamma and Integral Equation Method scattering models that are commonly utilized within the RF community for modeling bi-static scattering of material surfaces. Additionally, commonly utilized EO/IR reflectance and emissivity models are also available, such as a generic, spectrally interpolated micro-facet based polarized BRDF model (may be configured as a modified Beard-Maxwell model), a spectrally modulated Lambertian reflectance, and others utilized by the computer graphics community such as the Phong and Ward BRDF models.

One of the challenges existing within this development effort is translating class level (ie. Trees, buildings) reflectance properties to feature-level facetized surfaces (ie. leaves, branches, individual bricks). Work is currently underway to reconcile what feature-level scattering properties best represent class level measurements.

2.4 Atmosphere

DIRSIG has three options for simulating the atmospheric effects on SAR imaging. There is legacy support for the FASCODE model which supports RF atmospheric simulation. However, our understanding is FASCODE is no longer being developed and supported by the original authors. However, the radiative transfer code monoRTM is being actively developed by Atmospheric and Environmental Research (AER) Incorporated. The FORTRAN code for this product is available for free download [3] and utilizes the latest HITRAN 2000 line parameter database. monoRTM does a full line by line (as opposed to a band-model approximation) radiative transfer of visible thru RF radiation through the atmosphere. The standard MODTRAN style atmospheres are available within this code, such as mid-latitude summer and 1976 US Standard, permitting consistency with EO/IR simulations. The RF radiance from the sky is negligible in the RF region of the electromagnetic spectrum; therefore DIRSIG only currently utilizes monoRTM to determine transmission as a function of frequency.

For users lacking access to external radiative transfer codes such as FASCODE or monoRTM, the user has access to an internal atmospheric spectral transmission model applicable to simulations from 4 to 40GHz that is based on the empirical relationships reported on recently by Richards [7]. This model is based upon a collection of attenuation coefficients due to the primary atmospheric constituents (O2, H20), clouds, and rain. The plot in Figure 3 shows the derived atmospheric transmission of a space to ground path for a mid-latitude summer profile. The effects of the atmosphere on the coherency of transmitted and received waveforms is not currently supported, but will be investigated in future work.

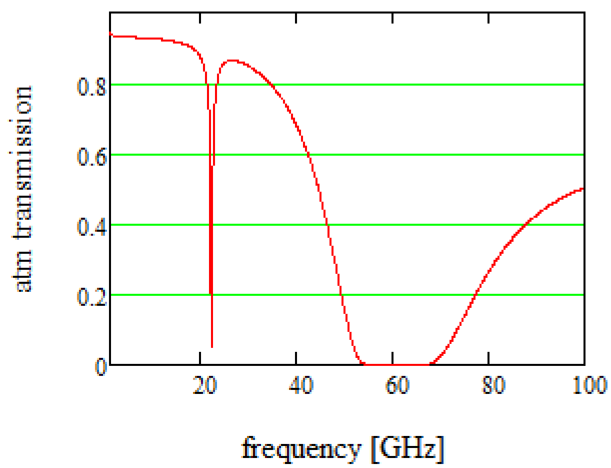

Figure 3. Atmospheric transmission profile as a function of frequency for a MLS atmosphere configuration.

2.5 Spatial Sampling

The nature of SAR signal collection and subsequent image focusing requires coherency (knowing the absolute phase in time and space) of the received pulses for each pulse. Non-SAR active imaging (such as LIDAR) typically does not hold this requirement, permitting a ray-tracing engine to sample arbitrary points in the scene in a non-consistent manner as long as they fall within the IFOV of a single pixel. If a SAR simulation is run that samples different points (although spatially on the same surfaces) in a scene between pulses, the resulting phase differences at the receive antenna will be due to both true path differences as well as spatial shifts from non-consistent sampling (Figure 4). This is a non-starter for attempting SAR simulations using existing DIRSIG active imaging techniques. Therefore, a crucial requirement for getting SAR simulations to put out accurate antenna level signals permitting image focusing in post-processing was to force coherency of sampled scene points between pulses. In reality, the transmitted photons are thought of as spatially continuous waves, not infinitely small particles as the simulation treats them.

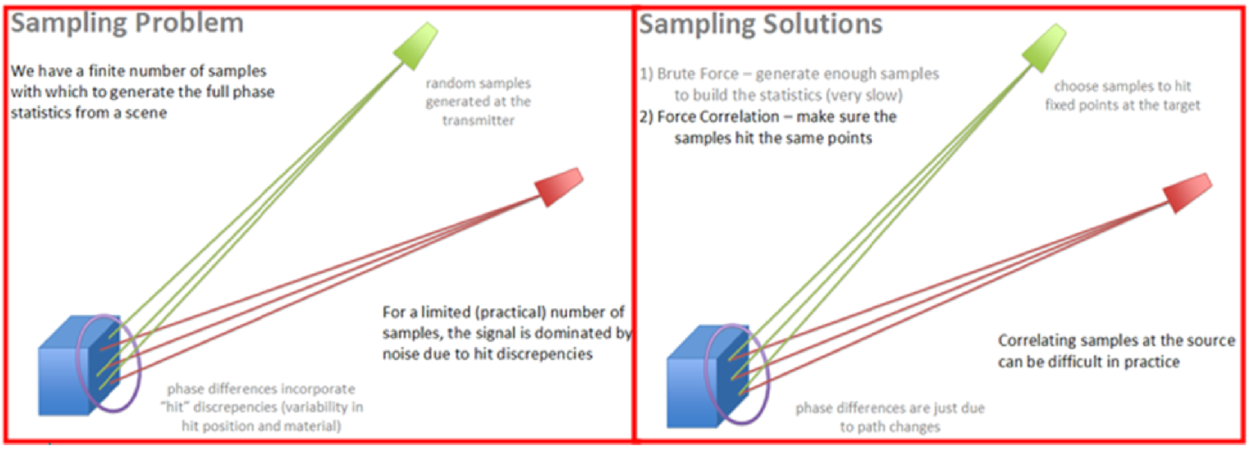

Figure 4. Schematic showing the nature of the coherency problem and two general approaches to a solution.

In a perfect world, DIRSIG could utilize its conventional particle based method of sampling the scene with an infinite number of photon samples to approximate the spatial extent of a continuous wave and preserve pulse-to-pulse coherency. However, practical computational considerations require finite amounts of sampling (on the order of 50,000 to 500,000 photon samples per pulse across the entire angular extent of the transmitted waveform). Therefore, we require a new approach to force coherency between pulses.

Our first approach looked at the obvious and easy solution of taking each photon intersection point and moving it to a global three dimensional, uniformly gridded post (see Figure 5). For example, if we choose global posting at a 0.5 meter level, an intersection point of (1.24, 0.34, -0.09) would get changed to (1.0, 0.5, 0.0). A subsequently transmitted pulse may hit an intersection point on the object that is very close, but not exactly so, of (1.21, 0.33, 0.01) which would again get changed to (1.0, 0.5, 0.0) maintaining coherency. However, there are a few issues with this approach. First off, forcing all intersection points to lie on 3D global posts will create intersection point not residing on any particular scene surface, but simply floating in space above or below an object surface. This may not be an issue with some larger objects, however for smaller objects this could severely deform the object appearance in the resulting focused SAR imagery. This approach was useful for proving a concept of getting the SAR capability to work, but not useful for serious simulations.

Our next approach investigated a modification of the original posting technique, but forcing the posts to reside on object surfaces. Therefore, the question arised as to how to create a near uniform type grid on an object surface. For this we chose a barycentric point generation approach (Figure 6) with customizable quantization levels. The barycentric approach works on the idea that you can take a triangular facet and break it into N approximately equal, but smaller triangular facets. The verticies of the facets become the new scene intersection posts forcing pulse to pulse coherency. Early tests of the sampling technique demonstrated some improvement in object appearance artifacts relative to original global 3D post approach by maintaining intersections on the actual surfaces, but turned out to uncover a Young's double slit type interference pattern as the platform moved along its path. In other words, when the intersection posts are close to being uniformly sampled, perfect broadside imaging shows great results. But as the platform begins to point either slightly forward or slightly back (such as in a spotlight mode collection) the intensity of the received signal actually modulated from bright to dark at the exact look angles predicted by the Young's double slit experiment.

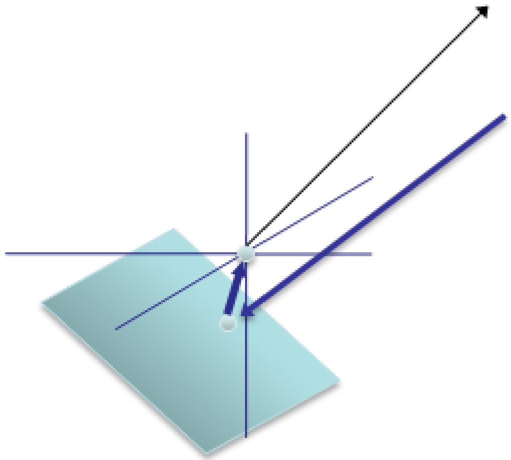

Figure 5. A initial attempt at efficient pulse to pulse coherency involved taking each intersection point and translating it to the nearest 3D regularly gridded post.

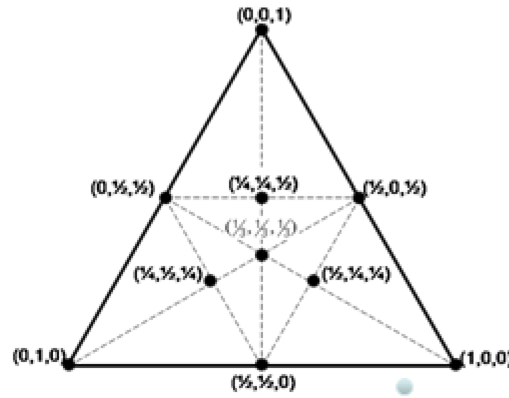

Figure 6. Another attempt at an efficient coherency preserving spatial sampling technique involved facet level quantization using a barycentric 2D posting scheme.

To solve this moving platform related sampling constructive and deconstructive interference issue, we looked into another sampling approach that attempted to randomize the locations of the hit points, but still maintain coherency. We chose to leverage the Monte Carlo nature of how DIRSIG samples the scene with photons by recording the intersection locations of many of the first shot photons and not adjusting their position to a mathematically predetermined 3D post, but simply do a Euclidean distance check to nearby posts. If subsequently shot photons were farther than a threshold distance away from previous intersection points, then their location was left intact. However if their distance to previous intersected locations was below a threshold, then their location was moved to that closest previously intersected point. The result is a random distribution of scene sample locations that can be maintained between pulses, but are random enough to produce roughly the same level of constructive and destructive interference as the platform moves along. In particular, if sub-apertures of a spotlight mode collection are focused, the overall intensity of the objects will stay the same, however a temporal speckle type pattern emerges demonstrating the path length and platform view angle dependence of the interference patterns generated by the clustered 3D intersection points.

Figure 7 demonstrates our current spatial sampling approach by showing red points where the original photons hit an object surface, each more than a specific distance threshold from each other. The last photon is rainbow colored to draw attention to the fact that the intersection point has a distance less than the threshold to a previous intersection point and is therefore shifted in position to that previous point.

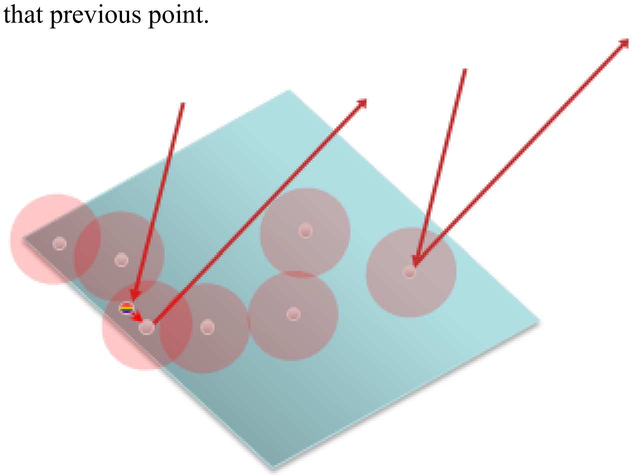

Figure 7. The current coherency preserving spatial sampling implementation is a thresholded facet level Eucleidian distance test.

An example of the real part of the DIRSIG generated complex phase history antenna signal, and the resulting focused SAR image, is shown below in Figure 8. This example assumed a simple unity reflectance, Lambertian shaped surface reflectance for both the target and background. RIT has written IDL-based algorithms for processing either spotlight-mode or stripmap-mode DIRSIG simulated complex phase history signals into exploitable imagery.

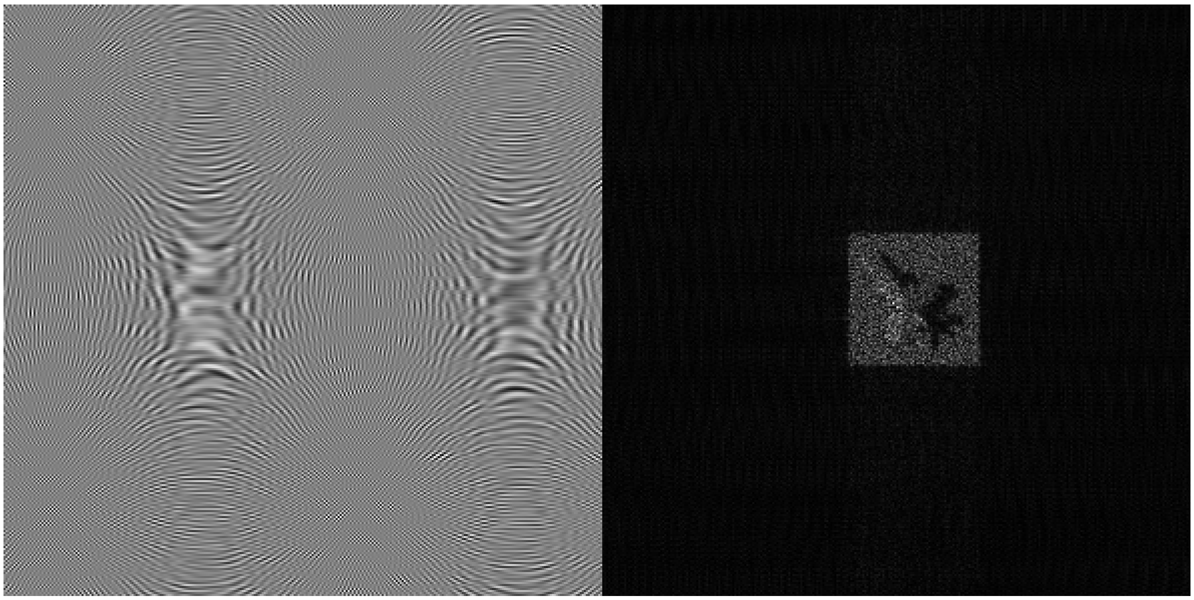

Figure 8. (left) Real part of DIRSIG phase history and (right) focused SAR image using IDL-based spotlight processor code.

3. RESULTS

The spatial sampling approach research is best summarized by presenting imagery focused from simulated SAR signals using each of the three coherency preserving spatial sampling approaches. The image in the left of Figure 9 shows the fighter jet target well, but has artifacts related to the uniform nature and off the surface nature of the chosen global 3D posts. The image in the middle shows a slight improvement by keeping the intersection points on the target surface, and adding a bit of non-unformity to the sampling scheme, however the dark region near the noise of the jet is resulting from coherent interference based on the sampling points determined for that region of the object. As the platform moves along its path and images the same target (such as with a spotlight mode collection) different areas of the jet will go in and out of focus and brightness demonstrating this sampling approaches shortfall. The image in the right hand side of Figure 9 shows a fighter jet sampled utilizing the current approach which preserves the random nature of how DIRSIG shoots photons onto the scene, but still maintaining pulse to pulse coherency permitting image focusing.

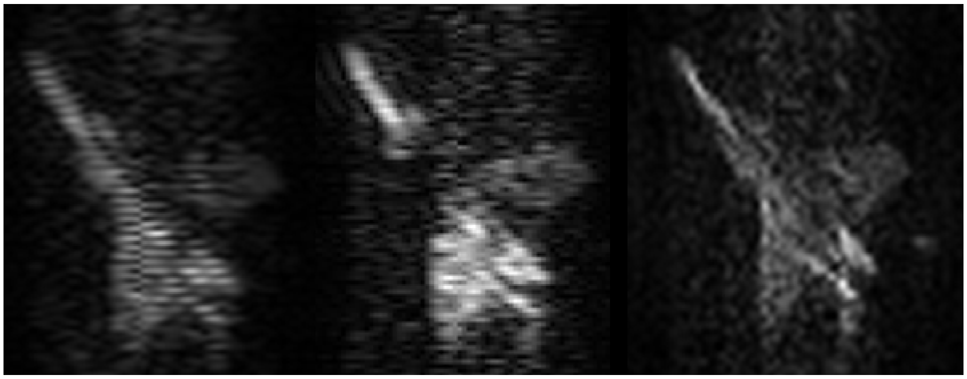

Figure 9. Focused SAR images of a fighter jet simulated using (left) original 3D global sampling posts, (middle) barycentric surface level quantization and (right) a Monte Carlo intersection post generation.

The current location for the spatial quantization of the scene intersection points is at the capture level, not the object intersection level which makes multiple bounce photon coherency challenging. Future work will move the spatial sampling approach to the intersection level (no dependence on photon bounce generation) to remedy this problem.

Another demonstration of the proposed spatial sampling technique utilizes a platform operated with similar transmit and receive antenna parameters, but operated in either spotlight or stripmap collection modes.

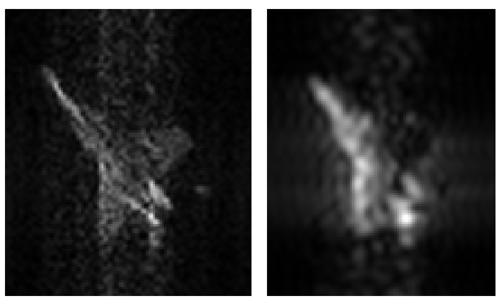

Figure 10. Focused spotlight (left) and stripmap (right) images of a fighter jet on a non-reflecting, flat background.

Still another example shows a series of collections (Figure 11) with different antenna parameters over a portion of RIT's Megascene 1, which is an urban scene that has a spatial extent of about 3 x 5 km in its entirety. This figure is a great demonstration of the computational challenge presented by modeling a spotlight SAR collection as a particle-based, ray-tracing process.

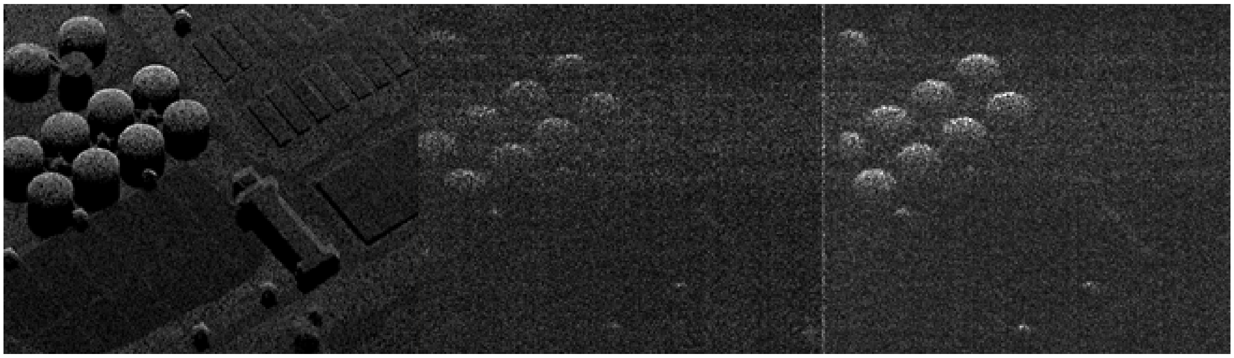

Figure 11. (left) Physically un-realizable real aperture RADAR image, (middle/right) and spotlight SAR images of the Van Lare plant portion of RIT's Megascene1.

A final example shows a single, spotlight SAR image over a residential neighborhood region of Megascene 1. The layover effects of the trees and homes are visible presenting an interesting clutter environment for placement of man-made targets in future simulations.

Figure 12. Focused spotlight SAR image of a portion of Megascene1 with grass, trees and a few homes within the field of view of the beam.

4. CONCLUSION

We have presented how RIT has begun to lay the core radiometric plumbing within the DIRSIG software for performing an accurate simulation of received Synthetic Aperture RADAR signals at the antenna level. We have provided a handful of options for propagation of RF waveforms through the atmosphere using either a hard coded attenuation model or an external line-by-line radiative transfer code monoRTM. Additionally we have adapted a few surface scattering models (in RCS form) from the RF literature into the particle ray-tracing world of photons and BRDF for use in RF simulations. Although hard-core diffraction effects are not yet implemented, some limited diffraction effects are captured within the context of the Physical Optics BRDF model. Additionally, we have demonstrated the capability of collected complex phase histories in both spotlight and stripmap SAR modes over simple target and background combinations as well as legacy DIRSIG scenes (i.e. Megascene 1). We have overcome some initial complications related to spatial sampling, but are still somewhat limited by knowing material properties at the facet level, whereas the RF literature describes them on the class level (ie. we need leaf BRDF versus tree and forest BRDF).

Challenges remain with the current state of the DIRSIG SAR simulation, namely (1) run times are large, (2) matching class level backscatter densities (related to BRDF) to facet level reflectance properties, and (3) improvement of multiple bounce coherency between pulses.

ACKNOWLEDGEMENTS

RIT would like to thank Lockheed Martin Information Systems and Global Services for partial funding of this work and technical feedback.

REFERENCES

[1] Michael Hazlett, Dennis J. Andersh, Shung W. Lee, Hao Ling, and C. L. Yu, “XPATCH: a high-frequency electromagnetic scattering prediction code using shooting and bouncing rays” , Proc. SPIE 2469, 266 (1995).
[2] Carla Willis, Charles Coker, Bea Thai, Omar Aboutalib, and John Pau., “Updates on fuze and SAR modes in RF channel for Irma 5.2 signature prediction model”, Proc. SPIE 7348, 734804 (2009)..
[3] http://rtweb.aer.com/monortm_frame.html, “monoRTM”, last accessed Oct 30, 2009.
[4] Garrido, E.E., “Graphical User Interface for a Physical Optics (PO) RCS Prediction code”, MS Thesis, Naval Postgraduate School, Monterey, CA, 2000, “http://www.dcjenn.com/pubs/ACESElmo.pdf”.
[5] John A. Richards, “Simulating the effects of long-range collection on synthetic aperture radar imagery”, Proc. SPIE 7337, 73370E (2009).